J. Phys. B: At. Mol. Opt. Phys. **22** (1989) 445-458. Printed in the UK

Multiphoton single and double ionisation of strontium in the range 532–541 nm

Pierre Camus‡, Michael Kompitsas‡, Samuel Cohen‡, Cleanthes Nicolaïdes‡, Mireille Aymar§, Michèle Crance§ and Pierre Pillet§

‡ Theoretical and Physical Chemistry Institute, National Hellenic Research Foundation, 48 Vas. Constantinou Ave, Athens 11635, Greece

§ Laboratoire Aimé Cotton, Centre National de la Recherche Scientifique, bât.505, 91405 Orsay Cedex, France

Received 2 August 1988, in final form 4 October 1988

Abstract. By focusing an excimer pumped dye laser on an atomic beam, we have observed multiphoton multiple ionisation of the neutral strontium atom in the tuned wavelength range 532-41 nm. Sr^+ and Sr^{++} yields were measured with a time of flight spectrometer. At least three photons are required to produce Sr^+ and eight photons to produce Sr^{++}. As a function of the wavelength, the Sr^+ yield exhibits resonances which correspond to two-photon excitation of bound states ($5s^2$-$5p^2\ ^1D_2$ and $5s^2$-$5p^2\ ^1S_0$) and three-photon excitation of autoionising states 4d5f $J=1$ and $J=3$ of the neutral atom. The Sr^{++} yield exhibits four broad smooth resonances that we interpret, from known spectroscopic data, as two-photon ($5p_{1/2}$-4f), three-photon ($5s$-$6p_{1/2,3/2}$) and four-photon (5s-7d) resonances in the singly charged ion. The latter transitions start from a singly charged ion in the 5s or $5p_{1/2}$ state reached after three- or four-photon ionisation of the neutral ground state. The variation of the Sr^{++} pattern as a function of the dye laser beam intensity shows that resonances are shifted and broadened when the intensity is increased. These features have been interpreted by a perturbative treatment of Sr^+ ionisation based on the use of an effective Hamiltonian which takes into account higher-order terms involved in the calculation of resonance effects. Calculated multiphoton ionisation probabilities are in good agreement with experimental data.

1. Introduction

We report new results on multiphoton multiple ionisation of the strontium atom in the range 532-41 nm. Single ionisation of strontium has previously been observed with a dye laser tuned in the ranges 556-64 nm (Chin *et al* 1981), 555-77 nm (Feldmann and Welge 1982) and 530-6 nm (Feldmann *et al* 1982a). Double ionisation, which requires stronger intensity (>40 GW cm^{-2}), was primarily investigated at a few fixed frequencies corresponding to the Nd:YAG laser (Aleksakhin *et al* 1979, Feldmann *et al* 1982a) and its harmonics (Feldmann *et al* 1982b). Double ionisation with tunable lasers was observed in a short range around 561 nm (Feldmann *et al* 1982), at low resolution between 562 and 592 nm (Bondar *et al* 1986) and recently from 558 to 570 nm with a picosecond dye laser (Agostini and Petite 1985a, b). A theoretical interpretation of the latter work has been given by Lambropoulos *et al* (1988). To our knowledge, double ionisation of strontium had never been observed in the range 532 to 541 nm.

† On leave from Laboratoire Aimé Cotton, Orsay, France.

0953-4075/89/030445+14$02.50

In § 2 we briefly recall the experimental set-up which has been presented elsewhere. Resonances observed in single ionisation yield have allowed us to identify autoionising levels never observed before. The spectra of ion yields are described in § 3. Resonances observed in double ionisation yield have been studied as a function of light intensity in order to ascertain their interpretation. The principles of the theoretical treatment are reviewed in § 4. The evolution of ion yield is discussed in § 5.

2. Experimental set-up

The experimental approach that we have used is pulsed dye laser multiphoton ionisation of Sr atoms in an atomic beam with a time of flight discrimination between Sr^+ and Sr^{++} ions. The experimental set-up is similar to the one used earlier to investigate double Rydberg autoionising levels in barium (Camus *et al* 1985). An effusive collimated beam produced by a resistively heated oven propagates between two parallel 90% transmission grids, 1 cm apart. The strontium beam density, where the laser is focused, is of the order of 10^9 cm^{-3}.

In order to generate light tunable in the range 532–41 nm, we use a 150 mJ XeCl excimer laser to pump a Coumarine 307 dye laser which produces pulses of frequency width 4.2 GHz (FWHM), duration 7.5 ns (FWHM) and energies up to 2 mJ (measured at the entrance window), at a 10 Hz repetition rate. The dye laser beam is focused by a spherical lens of 50 mm focal length between two grids, where it crosses the atomic beam at right angles. Direct observation of the laser beam at the focus was not possible and therefore we could not determine accurately the spatial distribution of intensity in the beam. It is reasonable to consider that the maximum intensity is in the range 8–16 GW cm^{-2}, these values being obtained under two extreme assumptions for the structure of the laser beam: a plane wave and a Gaussian beam respectively.

Approximately 200 ns after the laser is switched on, a static electric field pulse (200 V, 250 ns) is applied to one of the grids. The effect is to pull the ions out of the interaction volume towards a tandem of microchannel plates through a 10 cm long field free drift zone. The Sr^{++} and Sr^+ times of flight are respectively 10 and 20 μs. The two ion signals can be analysed simultaneously with a two-channel boxcar averager.

3. Spectroscopic interpretation of ion yields

The spectra of singly and doubly charged ions have been recorded as a function of laser wavelength. Resonances have been assigned to levels of neutral and singly ionised strontium respectively. A scheme of energy levels is given in figure 1. Resonance line wavelengths in ion yield spectra are measured by comparison with a one-photon optogalvanic spectrum provided by a commercial Ne hollow-cathode lamp used as a secondary standard for wavelength calibration. The accuracy of the laser wavelength measurements is of the order of 0.02 nm depending on the width of the lines.

3.1. Singly charged ions

Figure 2 shows the Sr^+ yield spectrum recorded with a linearly polarised dye laser beam. The upper trace is the Ne hollow-cathode OG spectrum which provides wavelength calibration. The lower trace is the Sr^+ yield spectrum. The strongest line

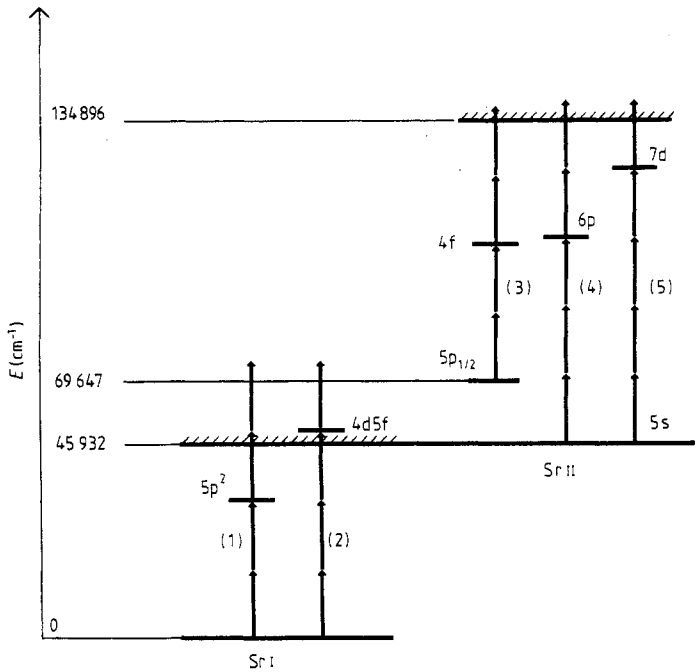

Figure 1. Schematic diagram energy levels in Sr and Sr^+ showing the multiphoton absorption mechanisms responsible for resonances observed in ion yields. (1) two-photon transitions $5s^2$-$5p^2\ ^1S_0$, $^1D_2$ in Sr^+ yield; (2) three-photon transitions $5s^2$-4d5f $J = 1, 3$ in Sr^+ yield; (3) two-photon transitions $5p_{1/2}$-$4f_{5/2,7/2}$ in Sr^{++} yield; (4) three-photon transitions $5s_{1/2}$-$6p_{1/2,3/2}$ in Sr^{++} yield; (5) four-photon transitions $5s_{1/2}$-$7d_{3/2,5/2}$ in Sr^{++} yield.

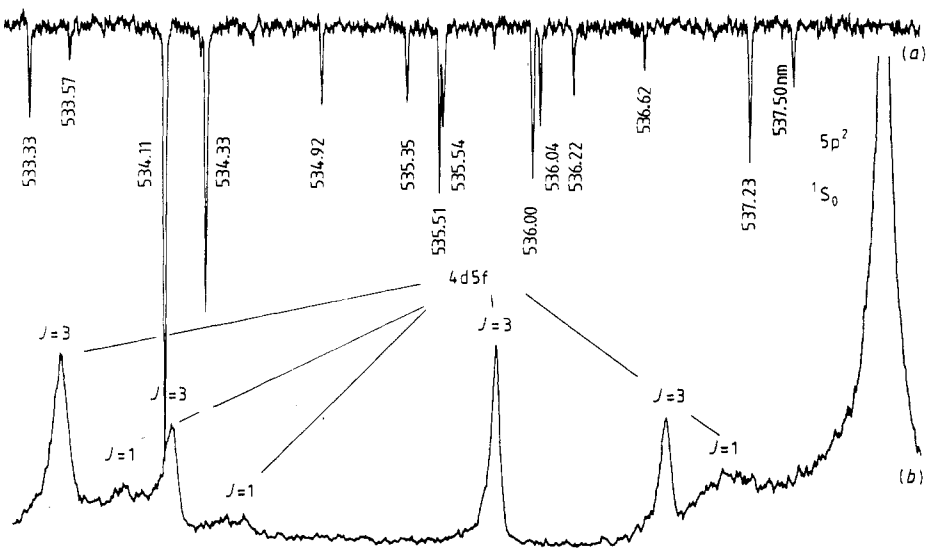

Figure 2. Sr^+ yield spectrum between 533 and 538 nm with linearly polarised light: (*a*) Ne hollow-cathode OG spectrum for wavelength calibration; (*b*) Sr^+ signal as a function of laser wavelength.

corresponds to a two-photon transition to bound level $5p^2\ ^1S_0$, the energy of which is given in Moore's tables (1947). The three weak and broad lines correspond to three-photon transitions to the 4d5f $J = 1$ autoionising levels previously observed in one-photon VUV absorption experiments (Garton and Codling 1968). The four medium and relatively sharp lines have been assigned to three-photon transitions to 4d5f $J = 3$ newly observed autoionising levels.

The latter assignments are confirmed by the variation of the Sr^+ pattern when the light polarisation is varied (see figure 3). In this perspective, we have carried out two series of experiments using either circular or linear polarisation with a lens of a longer focal length (200 mm). However, the polarisation is not completely preserved when the laser beam is so tightly focused. As a result, thanks to selection rules, we are able to discriminate between states $J = 1$ and $J = 3$, the latter being favoured when the initial polarisation is circular. Figures 3(*a*) and (*b*) show the spectrum of the Sr^+ yield as a function of laser wavelength for initial linear and circular polarisation respectively.

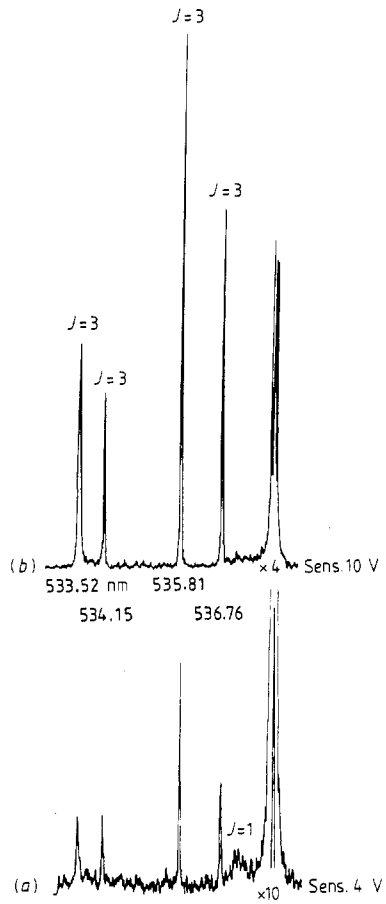

Figure 3. J level identification of the resonance lines in the Sr^+ spectrum allowed by the comparison of spectra recorded with: (*a*) linearly polarised laser beam (laser pulse energy: 1.8 mJ); (*b*) circularly polarised laser beam (laser pulse energy: 2 mJ). Note that for this particular recording the laser beam has been focused with a lens of 200 mm focal length in order to minimise depolarisation effects and make easier the recognition of selection rules.

Table 1. Observed resonances in the Sr^+ ion yield.

Observed wavelength (nm)	Observed wavenumber (cm^{-1})	Number of photons	Energy level (this work) (cm^{-1})	Identification	Energy level (other works) (cm^{-1})	Δ¶ (cm^{-1})
540.95	18 480.8	2	36 961.6	$5p^2\,{}^1D_2$	36 960.88†	+0.4
538.07	18 579.8	2	37 159.6	$5p^2\,{}^1S_0$	37 160.28†	−0.3
537.13	18 612.3	3	55 836.9	4d5f $J=1$	55 847.3‡	−3.5
536.76	18 625.1	3	55 875.3§	4d5f $J=3$		
535.81‖	18 658.1	3	55 974.3§	4d5f $J=3$		
534.48	18 704.6	3	56 113.8	4d5f $J=1$	56 107.7‡	+2
534.15‖	18 716.1	3	56 148.3§	4d5f $J=3$		
533.89	18 725.2	3	56 175.6	4d5f $J=1$	56 169.6‡	+2
533.32‖	18 738.2	3	56 214.6§	4d5f $J=3$		

† Moore's tables (1947).
‡ Garton and Codling (1968).
§ New identified levels.
‖ Observed previously by Feldmann *et al* (1982a) but not interpreted.
¶ Δ is the difference between wavenumbers measured in this work (second column) and wavenumbers deduced from previous measurements (sixth column).

The measured wavelengths, together with the assignment of the transitions, are listed in table 1.

3.2. Doubly charged ions

Figure 4 shows the Sr^{++} yield spectrum recorded with linearly (*a*) and circularly (*b*) polarised light ((*c*) will be commented upon later). In the range 18 200 to 18 800 cm^{-1} four broad resonances are observed. The pattern varies when the light intensity is varied and depends on the polarisation. As a function of light intensity, the two middle resonances, which are slightly shifted, can be assigned to a four-photon transition 5s-7d and a two-photon transition $5p_{1/2}$-4f. The two extreme resonances, which are strongly shifted when the intensity is increased, can be assigned to three-photon transitions $5s\text{-}6p_{1/2,3/2}$. These four resonances are much broader than the resonances observed in the Sr^+ yield. Profiles of the $5s\text{-}6p_{1/2,3/2}$ resonances are strongly asymmetric.

The difference in the Sr^{++} pattern for linear and circular polarisation confirms the assignments given above. $5s\text{-}6p_{1/2,3/2}$ transitions are forbidden in circular polarisation and appear in both spectra only because the initial polarisation of the light is not preserved after focusing ($f=50$ mm). A comparison of figures 4(*a*) and (*b*) shows that transition 5s-7d is favoured when the initial polarisation is circular.

In order to clarify the relation between the Sr^+ and Sr^{++} yield spectra, we have recorded both at the same intensity (0.9 mJ per light pulse). The Ne hollow-cathode OG spectrum is given for wavelength calibration (see figure 5).

4. Calculation of multiphoton ionisation probabilities

4.1. Principle of the method

We use the effective operator method which was initially introduced for the study of resonant multiphoton ionisation (Armstrong *et al* 1975) and has since been widely

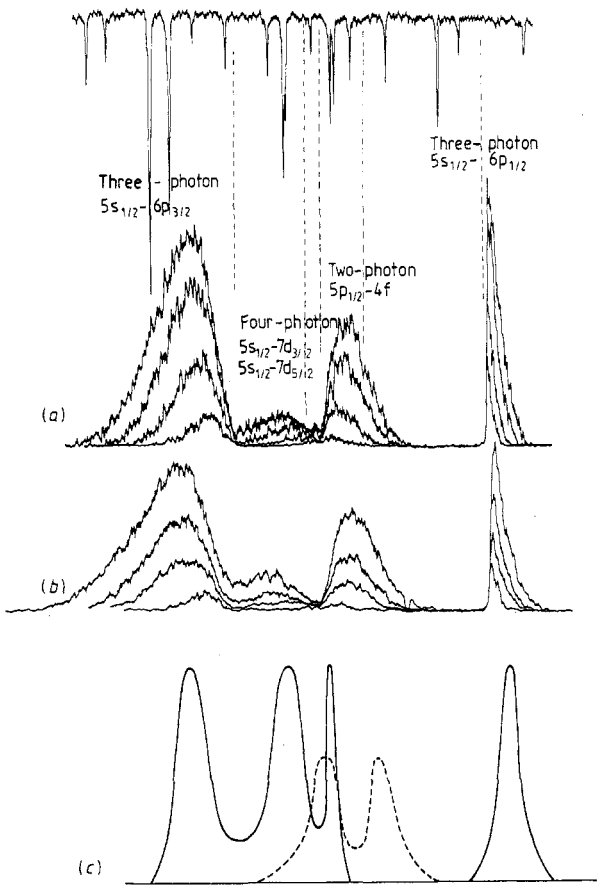

Figure 4. Sr^{++} yield spectrum for several pulse energies: (*a*) linearly polarised laser beam (laser pulse energies: 2.1, 1.6, 1.2 and 0.7 mJ); (*b*) circularly polarised laser beam (laser pulse energies: 2.2, 1.5, 1.1 and 0.55 mJ); (*c*) ionisation probability per light pulse calculated for intensity 15 GW cm^{-2} and pulse duration 7.5 ns. The broken lines are the calculated positions of the transitions from Moore's Tables (1947). For the recording corresponding to a pulse energy of 0.55 mJ, the signal has been multiplied by a factor of two.

used (Crance and Aymar 1980, Lompré *et al* 1980, Crance 1982, Petite *et al* 1984). The principle of the method consists in using the projection operator technique (Mower 1966) to define a set of discrete states for which an effective Hamiltonian is written. The Hamiltonian matrix elements (diagonal and non-diagonal) are calculated by standard perturbation treatment to the lowest non-vanishing order. Because of the ionisation processes, it is a non-Hermitian matrix. By diagonalisation of the effective Hamiltonian, eigenstates are defined by pseudoenergies; the real part corresponds to the energies, the imaginary part describes the relaxation of discrete states by photoionisation. In addition to the initial state, we introduce explicitly the discrete states which are expected to be strongly coupled with the initial state, i.e. the quasiresonant states at each step of the ionisation process.

We use the dressed-atom picture; the electromagnetic field is treated quantum mechanically. Dressed-atom states are tensorial products of atomic states and field states (in the occupation number representation). The initial state is $|i\rangle|N\rangle$ (N is

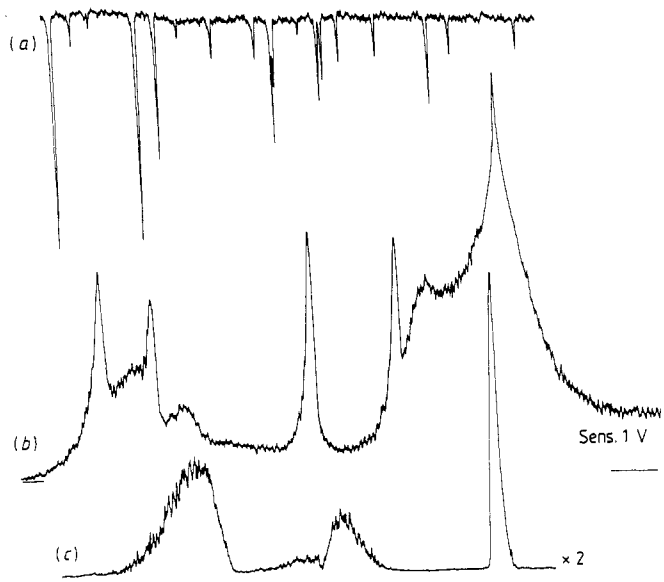

Figure 5. Sr^{+} and Sr^{++} yield spectra recorded for an energy of 0.9 mJ per light pulse with linearly polarised light: (*a*) Ne hollow-cathode OG spectrum for wavelength calibration; (*b*) Sr^{+} yield; (*c*) Sr^{++} yield.

assumed to be large and need not to be given an explicit value). A quasiresonant state is written as $|\alpha\rangle|N-r\rangle$ when the transition i-α involves r photon absorptions. Two types of matrix elements are involved: multiphoton transition probability amplitudes and non-resonant AC Stark shifts. The Hamiltonian matrix elements vary smoothly in the range of frequency where the light field can be put in resonance with the states explicitly introduced. We thus calculate the effective Hamiltonian matrix elements for a few frequencies in this range. By interpolating each matrix element, we obtain an analytic expression of the effective Hamiltonian matrix valid in a large range of frequency. Atomic quantities are computed in the framework of a single-electron model using a central potential (Klapisch 1971). The method described above has been applied to the five-photon ionisation from the singly charged ion of strontium in the state 5s and to the four-photon ionisation from Sr^{+} in the state $5p_{1/2}$ for linearly polarised light.

4.2. Five-photon ionisation from singly charged strontium in the state 5s

Ionisation of $Sr^{+}(5s)$ in the range 18 200 to 18 800 cm^{-1} requires the absorption of five photons. After absorption of three photons, there are two quasiresonant states: $6p_{1/2}$ and $6p_{3/2}$. After absorption of four photons, there are three quasiresonant states: 8s, $7d_{3/2}$ and $7d_{5/2}$. The Hamiltonian matrix is built on the six states $|5s\rangle|N\rangle$, $|6p_{1/2}\rangle|N-3\rangle$, $|6p_{3/2}\rangle|N-3\rangle$, $|8s\rangle|N-4\rangle$, $|7d_{3/2}\rangle|N-4\rangle$ and $|7d_{5/2}\rangle|N-4\rangle$. Up to a light intensity of 1 GW cm^{-2}, the ionisation probability from 5s hardly departs from its value obtained by perturbation treatment at lowest non-vanishing order, except very close to resonances. For larger intensities, the resonances are shifted. The 7d resonances which remain very close together are slightly shifted towards higher frequencies. The 6p resonances are shifted apart, more strongly for $6p_{3/2}$ than for $6p_{1/2}$. The results are given in figure 6. Resonances $6p_{1/2}$ and $6p_{3/2}$ are of similar magnitudes. Resonance

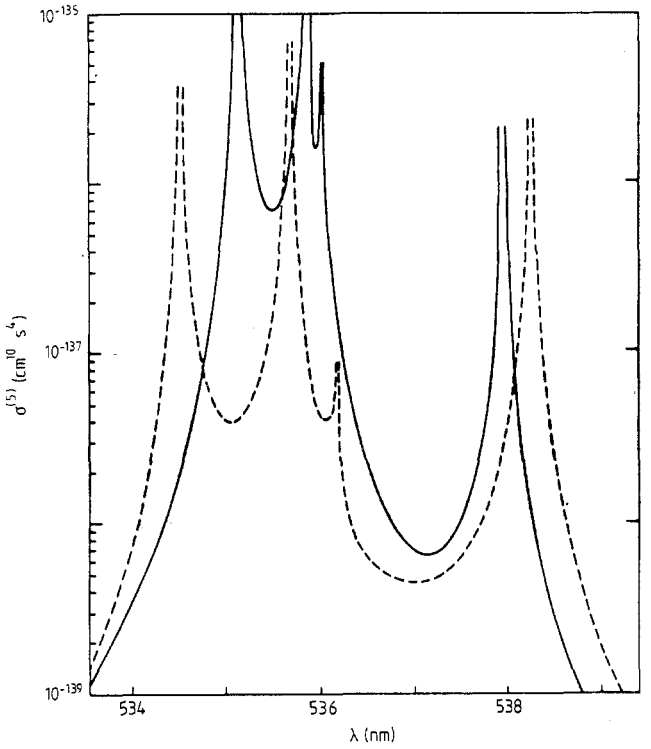

Figure 6. Intensity-dependent five-photon ionisation cross sections from the $5s_{1/2}$ state of Sr^+ for two intensities: full line, intensity lower than 1 GW cm^{-2}; broken line, intensity 15 GW cm^2. For increasing wavelength, resonances occur in the order $6p_{3/2}$, $7d_{5/2}$, $7d_{3/2}$, $6p_{1/2}$.

$7d_{3/2}$ is much smaller than resonance $7d_{5/2}$. The most important contributions to ionisation correspond to the paths involving resonant states. There is only one such path involving $7d_{5/2}$ (i.e. $5s\text{-}6p_{3/2}\text{-}7d_{5/2}$). There are two paths involving $7d_{3/2}$ (i.e. $5s\text{-}6p_{1/2}\text{-}7d_{3/2}$ and $5s\text{-}6p_{3/2}\text{-}7d_{3/2}$). These paths interfere destructively because their magnitudes are similar and their signs are opposite since 7d resonances fall between $6p_{1/2}$ and $6p_{3/2}$ resonances. This destructive interference explains the weakness of resonance $7d_{3/2}$.

4.3. Four-photon ionisation from singly charged strontium in the state 5p

Ionisation of $Sr^+(5p_{1/2})$ in the range 18 200 to 18 800 cm^{-1} requires the absorption of four photons. After absorption of two photons, there are two quasiresonant states: $4f_{5/2}$ and $4f_{7/2}$. The initial state $5p_{1/2}$ is strongly coupled to $5p_{3/2}$. The Hamiltonian matrix is built on the four states $|5p_{1/2}\rangle|N\rangle$, $|5p_{3/2}\rangle|N\rangle$, $|4f_{5/2}\rangle|N-2\rangle$ and $|4f_{7/2}\rangle|N-2\rangle$. Up to a light intensity of 1 GW cm^{-2}, the ionisation probability from $5p_{1/2}$ hardly departs from its value obtained by perturbation treatment at lowest non-vanishing order. For larger intensities, the resonances are slightly shifted towards low frequencies. The results are given in figure 7.

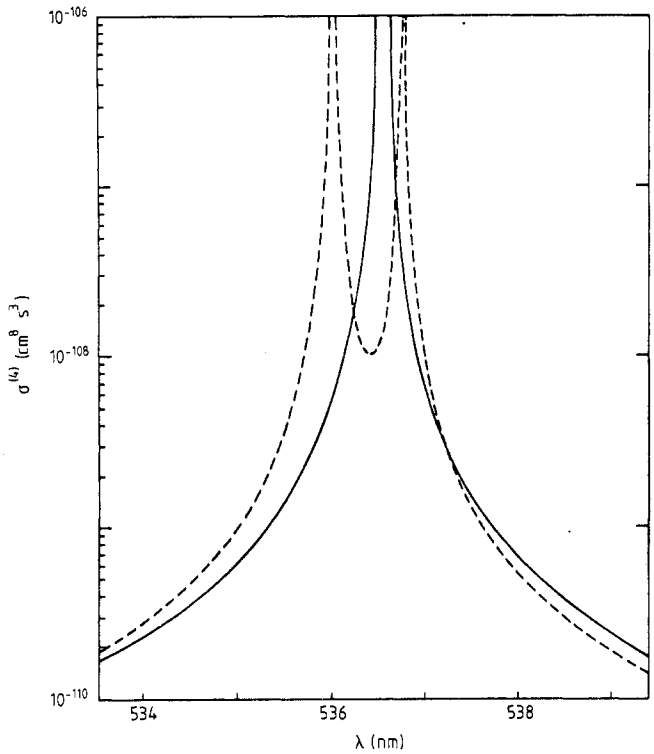

Figure 7. Intensity-dependent four-photon ionisation cross section from the $5p_{1/2}$ state of Sr^+ for two intensities: full line, intensity lower than 1 GW cm^{-2}; broken line, intensity 15 GW cm^{-2}.

5. Interpretation of the ion yields

The number of singly and doubly charged ions have been measured as a function of the laser frequency for various intensities. Ions are detected with a time of flight spectrometer, so that it is not possible to know in which state the ions are produced. Concerning doubly charged ions, there is no ambiguity since the first excited state of Sr^{++} is located at least 100 000 cm^{-1} above the ground state. For singly charged ions, there is certainly a large number of ions produced in excited states 4d and 5p. This belief is based first on the knowledge of the electron energy spectrum, which has been studied by Agostini and Petite (1985a, b) for a frequency range very close to the one concerned here. The analysis of the electron energy spectrum allowed them to determine how many photons were absorbed and what the state of the singly charged ion formed was. It appeared that a large proportion of the events (more than 50%) leads to the formation of Sr^+ in an excited state (4d or 5p). These features are confirmed by the results obtained for the Sr^{++} yield. When we compare the Sr^+ and Sr^{++} ion yields in figure 5, it is clear that the thin resonances observed in the Sr^+ yield have no counterpart in the Sr^{++} yield, which consists of wide smooth resonances. Because of these observations, we propose an interpretation based on a qualitative analysis of Sr multiphoton ionisation and a quantitative analysis of multiphoton ionisation of Sr^+ either from state 5s or from state $5p_{1/2}$ (ionisation from state 4d does not contribute

efficiently to ionisation in the range of frequencies investigated). In order to interpret the development of resonances, we need to recall some general features about resonant multiphoton ionisation in strong fields.

5.1. Resonant multiphoton ionisation: general features

The intensity dependence of multiphoton ionisation near a resonance has been widely studied and we shall only recall the essential features. For n-photon ionisation, r-photon resonant, the width of the resonance is the ionisation probability from the resonant state, and thus it increases as the $(n-r)$th power of intensity. The area under the resonant profile grows as the rth power of intensity and thus the magnitude of the resonance at its maximum increases as the $(2r-n)$th power of intensity. The background ion yield $N(Sr^+(5s))$ is expected to increase as the third power of intensity. Obviously, the latter considerations are valid when ionisation is not saturated, i.e. when the number of ions created remains small compared to the number of neutrals available. When saturation occurs, the ionisation probability remains constant when the intensity is increased. The number of ions created increases because of the extension of the interaction volume: a larger number of atoms are irradiated by a light field able to saturate ionisation. Saturation occurs first at the maximum of resonance profiles. When the intensity is increased, the width of the profile is no longer the ionisation probability of the resonant state.

5.2. Analysis of multiphoton ionisation of neutral strontium

In the range of frequencies where doubly charged ions of strontium are observed (18 560 to 18 750 cm^{-1}), the neutral strontium ground state ionises after absorption of at least three photons. The observed Sr^+ yield is the sum of the yields $Sr^+(5s)$, $Sr^+(5p)$ and $Sr^+(4d)$. In order to interpret the formation of doubly charged ions, we have to understand what are the relative contributions to $Sr^+(5s)$, $Sr^+(5p)$ and $Sr^+(4d)$ respectively. The thin resonances observed in the Sr^+ yield do not appear in the Sr^{++} yield. This suggests that the yield of $Sr^+(5s)$ is a slowly varying function of frequency and that the resonances belong to $Sr^+(5p)$ or $Sr^+(4d)$.

Single ionisation to the 5s state requires the absorption of three photons while double ionisation from the 5s state requires the absorption of five photons. As a consequence, the saturation intensity for single ionisation in the 5s state is smaller than for double ionisation. It is thus reasonable to consider the yield of Sr^+ in the 5s state as constant in the range of frequencies where resonances are observed in Sr^{++} yield. The latter assumption is confirmed by the studies of intensity dependence discussed below. However, we have to keep in mind a possible smooth variation of the Sr^+ yield which would induce a distortion of the Sr^{++} spectrum.

5.3. Analysis of multiphoton ionisation of singly charged strontium

In the range of frequencies 18 560 to 18 750 cm^{-1}, four broad smooth resonances are obtained. The absence of any thin resonance in the yield of Sr^{++} confirms our interpretation of ionisation of neutral strontium: the resonances appearing in the Sr^+ yield belong to the yield of Sr^+ in an excited state but have a negligible contribution to the yield of Sr^+ in the ground state. From known spectroscopic data, the resonances

can be assigned to the transitions $5s\text{-}6p_{1/2}$, 5s–7d, $5p_{1/2}\text{-}4f$ and $5s\text{-}6p_{3/2}$. The variation of the pattern as a function of light intensity shows that the resonances are shifted apart when the intensity is increased. This is due to the strong one-photon interaction between the 7d and 6p states. For isolated resonances, the light shift is generally a quadratic function of the intensity. For the more complex interactions occurring here, the intensity dependence of light shifts cannot be described by a simple analytical formula. Since the transitions $Sr \rightarrow Sr^{+} \rightarrow Sr^{++}$ occur sequentially, for each resonance $nl_j \rightarrow n'l'_{j'}$, the number of doubly charged ions detected, $N(Sr^{++})$, is the product of the number of singly charged ions $N(Sr^{+}(nl_j))$ produced and the ionisation probability from singly charged strontium in state nl_j. In order to obtain the ionisation probability, $P(Sr^{++}(nl_j))$, from state nl_j, we must 'renormalise' the resonance profiles by the ion yield $N(Sr^{+}(nl_j))$.

Experimentally, the light intensity has been varied from 0.1 I_M to I_M. Theoretical predictions for light shifts are in good agreement with experimental positions at maximum intensity I_M for an intensity of about 15 GW cm^{-2}. This value is compatible with the experimental determination of the light intensity. The comparison between experimental profiles and theoretical curves of ionisation probability shows that the transitions $5p_{1/2} \rightarrow 4f$, $5s \rightarrow 6p_{1/2}$ and $5s \rightarrow 6p_{3/2}$ are saturated. In other words the probabilities $P(Sr^{+}(5s) \rightarrow Sr^{++})$ and $P(Sr^{+}(5p) \rightarrow Sr^{++})$ both equal one at the maximum of each profile. The increase of $N(Sr^{++})$ with intensity is only due to the increase of the Sr^{+} yield.

The intensity dependence of the ion yield has been measured, in the range 0.1 I_M to I_M (I_M corresponds to 2.2 mJ of energy per light pulse), on the top of resonances 4f, $6p_{1/2}$, $6p_{3/2}$ and on the wing of resonance $6p_{3/2}$. The curves, in a log–log plot, are approximately straight lines in the lowest range of intensity, then they bend near maximum intensity. According to the discussion of § 5.1, for low intensity we expect $P(Sr^{+}(5s) \rightarrow Sr^{++})$ to vary linearly with intensity at the top of resonances 6p ($r = 3$, $n = 5$ and thus $2r - n = 1$) and to be independent of intensity at the top of resonance 4f ($r = 2$, $n = 4$ and thus $2r - n = 0$). Our assumption of a frequency-independent Sr^{+} yield means, in fact, that we assume the processes $Sr \rightarrow Sr^{+}(5s)$ and $Sr \rightarrow Sr^{+}(5p)$ to be non-resonant. The latter assumption implies that, at least for low intensity, $P(Sr \rightarrow Sr^{+}(5s))$ varies as the third power of intensity and $P(Sr \rightarrow Sr^{+}(5p))$ varies as the fourth power of intensity. Finally, we expect the yield of Sr^{++} to vary as the fourth power of intensity at the top of resonances 4f, $6p_{1/2}$ and $6p_{3/2}$. This is compatible with the curves presented in figure 8. How fast the slope decreases when the intensity is increased, reflects the saturation of single ionisation. Saturation of single ionisation appears first at resonance $6p_{1/2}$ (for pulse energy 0.7 mJ) and then at resonances 4f and $6p_{3/2}$ (for pulse energy 1 mJ). The linear intensity dependence for intensity close to I_M means that both transitions $Sr^{+}(5s) \rightarrow Sr^{++}$ and $Sr \rightarrow Sr^{+}(5s)$ are saturated. The curve in figure 8(*d*) corresponds to the wing of resonance $6p_{3/2}$. This curve is to be interpreted with reference to figure 8(*c*). For the straight line part, the slope is larger in (*d*) than in (*c*). Such behaviour is expected since the slope for low intensity is known (Crance 1982) to vary from $2r - n$ to n for frequencies varying from the top of the resonance to the extreme wings of the profile. The intensity dependence observed confirms our interpretation for the respective roles of single and double ionisation.

For maximum intensity, the profile of the $6p_{3/2}$ resonance is about four times broader than the profile of the $6p_{1/2}$ resonance while our theoretical investigations predict similar magnitudes for the two components. Calculation of resonance profiles shows that, for saturated ionisation, only the wings of the profiles have to be considered.

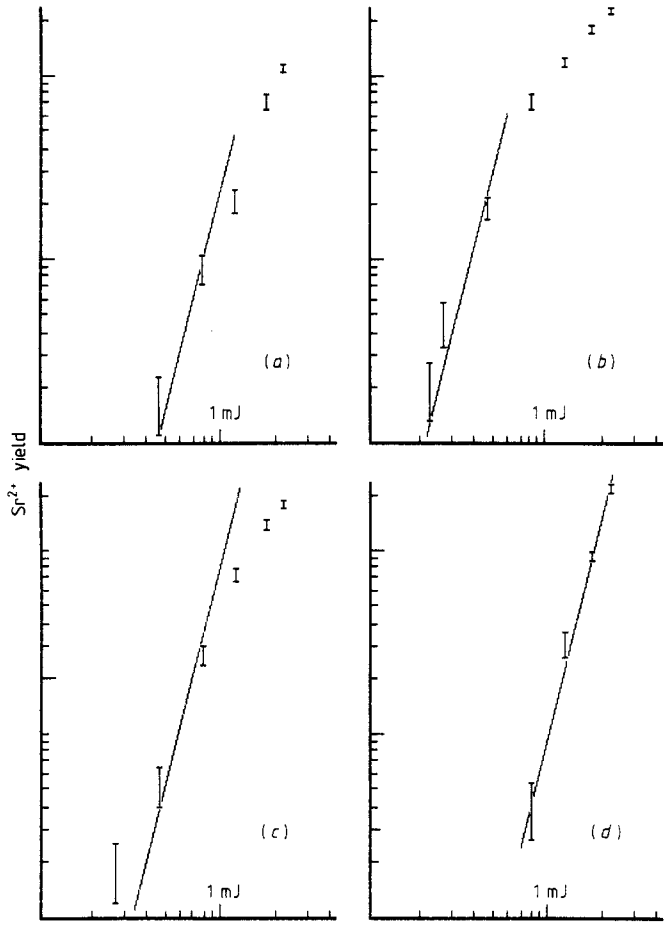

Figure 8. Log-log plot of double ionisation yield as a function of laser intensity for various frequencies: (*a*) top of resonance $5p_{1/2}$-4f; (*b*) top of resonance $5s_{1/2}$-$6p_{1/2}$; (*c*) top of resonance $5s_{1/2}$-$6p_{3/2}$; (*d*) High-frequency wing of resonancee $5s_{1/2}$-$6p_{3/2}$. A straight line of slope four has been drawn among the experimental points.

Under this assumption, the width of theoretical profiles for 6p resonances are in the ratio 1:4.

Starting from intensity-dependent multiphoton ionisation cross sections presented in figures 5 and 6, we have calculated the ionisation probability per light pulse for an intensity of 15 GW cm^{-2} and a pulse duration of 7.5 ns (see figure 4(*c*)). The number of singly charged ions $Sr^+(5s)$ and $Sr^+(5p_{1/2})$ has been chosen to fit the experimental value of Sr^{++} at the maximum of 6p and 4f resonances respectively. Theoretical profiles are not expected to fit experimental ones exactly, since in the calculation we have not taken into account the spatial and temporal distribution of intensity which is known to influence strongly the precise shape of resonances (Crance and Aymar 1980).

Calculation of 6p resonances is in good agreement with experimental profiles. The 7d resonance is overestimated by the calculation. This feature, and the strong asymmetry of experimental profiles for resonances with transitions starting from 5s, may be due to a slight decrease of the Sr^+ yield in the frequency range between the two

6p resonances. The calculated 4f resonance profile presents a dip which does not appear in experimental data. This feature can be understood from the results given in figure 6. The $4f_{5/2}$ and $4f_{7/2}$ states are strongly coupled with each other by the two-photon interaction. This results in a large AC Stark shift which essentially increases the doublet splitting without changing noticeably its centre of gravity. However, the dip in the resonance profile shifts when the intensity is increased. Consequently, if spatial and temporal distributions of intensity were taken into account, the doublet structure would vanish to give a broad resonance with a width of the order of the splitting at maximum intensity. From such considerations, we can conclude that the ionisation probability confirms the assignment of resonances in the Sr^{++} yield spectrum.

Excitation of resonances 6p, after absorption of three photons, and 7d, after absorption of four photons, is possible only for linearly polarised light. However, the light beam has an elliptic polarisation that we can treat as two independent components of an orthogonal polarisation. The largest component being taken as the polarisation axis, its effect is to produce multiphoton ionisation, as described and calculated above, through quantum paths corresponding to a constant value ($\pm\frac{1}{2}$) of the projection, m, of the total momentum, j, on the quantisation axis. The effect of the orthogonal component is to mix states with different values of m and open new ways to ionisation. The elliptic character of the polarisation of the light may be responsible for the discrepancy observed in the comparison of experimental and theoretical resonance profiles.

6. Conclusion

We have observed multiphoton multiple ionisation of strontium in the range 532–41 nm. Measurement of the Sr^{+} yield has allowed us to obtain accurate values for the energy of the four expected autoionising states 4d5f with $J = 3$. Resonances have been observed in the Sr^{++} yield, and their assignments were ascertained by accurate calculations of the ionisation probability which explicitly took into account strong field effects occurring near resonances.

The richness of the processes observed in the range of frequencies investigated shows that it would be interesting to complete the present study by electron measurements (energies and angular distributions). This case should constitute a favourable situation to test the various mechanisms expected to be responsible for double ionisation and, in particular, to discriminate between the direct and the stepwise processes which are involved.

Acknowledgments

This work has been supported in part by the Centre National de la Recherche Scientifique and the National Hellenic Research Foundation in the frame of an Exchange Visitor Program.

Note

After submission of this manuscript, a low-resolution experimental investigation was published by Bondar I I, Delone N B, Dudich M I and Suran V V 1988 *J. Phys. B: At. Mol. Opt. Phys.* **21** 2763.

References

Agostini P and Petite G 1985a *Phys. Rev.* A **32** 3800
—— 1985b *J. Phys. B: At. Mol. Phys.* **18** L281
Aleksakhin I S, Delone N B, Zapesochnyi I P and Suran V V 1979 *Sov. Phys.-JETP* **49** 447
Armstrong L Jr, Beers L B and Feneuille S 1975 *Phys. Rev.* A **12** 1903
Bondar I I, Dudich M I and Suran V V 1986 *Sov. Phys.-JETP* **63** 1142
Camus P, Pillet P and Boulmer J 1985 *J. Phys. B: At. Mol. Phys.* **18** L481
Chin S L, Feldmann D, Krautwald J and Welge K H 1981 *J. Phys. B: At. Mol. Phys.* **14** 2353
Crance M 1982 *Multiphoton Ionisation of Atoms* ed P Lambropoulos and S L Chin (Orlando, FL: Academic)
Crance M and Aymar M 1980 *J. Phys. B: At. Mol. Phys.* **13** 4129
Feldmann D, Krautwald J, Chin S L, von Hellfeld A and Welge K H 1982a *J. Phys. B: At. Mol. Phys.* **15** 1663
Feldmann D, Krautwald H J and Welge K H 1982b *J. Phys. B: At. Mol. Phys.* **15** L529
Feldmann D and Welge K H 1982 *J. Phys. B: At. Mol. Phys.* **15** 1651
Garton W R S and Codling K 1968 *J. Phys. B: At. Mol. Phys.* **1** 106
Klapisch M 1971 *Comput. Phys. Commun.* **2** 239
Lambropoulos P, Tang X, Agostini P, Petite G and L'Huillier A 1988 *Phys. Rev.* A to be published
Lompré L A, Mainfray G, Mathieu B, Watel G, Aymar M and Crance M 1980 *J. Phys. B: At. Mol. Phys.* **13** 1799
Moore C E 1947 *NBS Circular* no 467
Mower L 1966 *Phys. Rev.* **142** 799
Petite G, Fabre F, Agostini P, Crance M and Aymar M 1984 *Phys. Rev.* A **29** 2677